THE JOURNAL OF BIOLOGICAL CHEMISTRY VOL. 283, NO. 44, pp. 30363–30375, October 31, 2008

Up-regulating Sphingosine 1-Phosphate Receptor-2 Signaling Impairs Chemotactic, Wound-healing, and Morphogenetic Responses in Senescent Endothelial Cells*[S]

Received for publication, June 6, 2008, and in revised form, August 21, 2008 Published, JBC Papers in Press, September 2, 2008, DOI 10.1074/jbc.M804392200

Rosendo Estrada[‡], Qun Zeng[‡], Hongwei Lu[‡], Harshini Sarojini[‡], Jen-Fu Lee[‡], Steven P. Mathis[§], Teresa Sanchez[¶], Eugenia Wang[‡], Christopher D. Kontos[‖], Chen-Yong Lin[**], Timothy Hla[¶], Bodduluri Haribabu[§], and Menq-Jer Lee[‡§1]

From the [‡]Gheens Center on Aging, University of Louisville Health Sciences Center, Louisville, Kentucky 40202, the [§]Department of Microbiology and Immunology, University of Louisville Health Sciences Center, Louisville, Kentucky 40202, the [¶]Center for Vascular Biology, University of Connecticut Health Center, Farmington, Connecticut 06030, the [‖]Department of Medicine, Division of Cardiology, and Department of Pharmacology and Cancer Biology, Duke University Medical Center, Durham, North Carolina 27710, and the [**]Greenebaum Cancer Center, Department of Biochemistry and Molecular Biology, University of Maryland School of Medicine, Baltimore, Maryland 21201

Vascular endothelial cells (ECs) have a finite lifespan when cultured *in vitro* and eventually enter an irreversible growth arrest state called "cellular senescence." It has been shown that sphingolipids may be involved in senescence; however, the molecular links involved are poorly understood. In this study, we investigated the signaling and functions of sphingosine 1-phosphate (S1P), a serum-borne bioactive sphingolipid, in ECs of different *in vitro* ages. We observed that S1P-regulated responses are significantly inhibited and the $S1P_{1-3}$ receptor subtypes are markedly increased in senescent ECs. Increased expression of $S1P_1$ and $S1P_2$ was also observed in the lesion regions of atherosclerotic endothelium, where senescent ECs have been identified *in vivo*. S1P-induced Akt and ERK1/2 activation were comparable between ECs of different *in vitro* ages; however, PTEN (phosphatase and tensin homolog deleted on chromosome 10) activity was significantly elevated and Rac activation was inhibited in senescent ECs. Rac activation and senescent-associated impairments were restored in senescent ECs by the expression of dominant-negative PTEN and by knocking down $S1P_2$ receptors. Furthermore, the senescent-associated impairments were induced in young ECs by the expression of $S1P_2$ to a level similar to that of *in vitro* senescence. These results indicate that the impairment of function in senescent ECs in culture is mediated by an increase in S1P signaling through $S1P_2$-mediated activation of the lipid phosphatase PTEN.

Spingosine 1-phosphate (S1P),[2] a serum-borne bioactive lipid mediator, regulates an array of biological activities in various cell types (1–4). Most, if not all, of S1P-regulated functions are mediated by the S1P family of G-protein-coupled receptors (GPCRs) (5–7). There are five identified members of the S1P receptor family: $S1P_1$, $S1P_2$, $S1P_3$, $S1P_4$, and $S1P_5$ (old nomenclature: EDG-1, -5, -3, -6, and -8, respectively) (8). It was demonstrated that S1P receptor subtypes couple to different G_α polypeptides to regulate distinct signaling pathways (9–11). The S1P receptor subtypes were expressed in distinct combinations in different cell types to produce an appropriate biological effect. For example, $S1P_1$ and $S1P_3$ are expressed in endothelial cells (ECs) (12). The signaling pathways regulated by the $S1P_1$ and $S1P_3$ receptors are required for the chemotaxis of endothelial cells, adherens junction assembly, endothelial morphogenesis, and angiogenic response *in vitro* and *in vivo* (7, 12–13). However, the functional outcomes resulting from the concerted effects of the signaling pathways mediated by the distinct S1P receptor subtypes are currently unknown in a physiological environment.

In contrast to $S1P_1$-stimulating chemotaxis, $S1P_2$-mediated signaling was shown to inhibit cell migration (14–16). For example, embryonic fibroblasts isolated from $S1P_2$ null mice exhibited an enhanced chemotaxis toward S1P, serum, and platelet-derived growth factor; this enhancement was reversed by the reintroduction of $S1P_2$ receptors (14). Recently, the mechanisms of $S1P_2$-regulated inhibition of chemotaxis have started to become identified in several laboratories. For example, it was shown that the inhibition of migration by the $S1P_2$ receptor was mediated by $G_{\alpha 12/13}$-dependent Rac inactivation (15). In addition, Rho-dependent PTEN activation was demonstrated to account for the $S1P_2$-mediated inhibitory effect (16). Together, these data indicate that S1P is able to control two completely opposite biological activities via the activation of distinct S1P receptor signaling pathways, *i.e.* $S1P_1$ stimulates

* This work was supported, in whole or in part, by National Institutes of Health Grant R01HL071071 (to M. L). This work was also supported by American Heart Association Grant-in-Aid 0755245B (to M. L.). The costs of publication of this article were defrayed in part by the payment of page charges. This article must therefore be hereby marked "*advertisement*" in accordance with 18 U.S.C. Section 1734 solely to indicate this fact.

[S] The on-line version of this article (available at http://www.jbc.org) contains supplemental Fig. S1.

[1] To whom correspondence should be addressed: University of Louisville Health Sciences Center, 580 S. Preston St., Louisville, KY 40202. Tel.: 502-852-7729; Fax: 502-852-2660; E-mail: menqjer.lee@louisville.edu.

[2] The abbreviations used are: S1P, sphingosine 1-phosphate; GPCR, G-protein-coupled receptor; $S1P_1$ and $S1P_2$ (old nomenclature EDG-1, endothelial differentiating gene-1, and EDG-5, respectively), two high affinity GPCRs for S1P; PTEN, phosphatase and tensin homolog deleted on chromosome 10; WT- and DN-PTEN, wild-type and dominant-negative PTEN constructs (PTEN-C/S, the catalytic Cys-124 is mutated to Ser); FAK, focal adhesion kinase; TEER, transendothelial electrical resistance; ECIS, electrical cell-substrate impedance-sensing technique; HUVEC, human umbilical vein endothelial cell; EC, cultured endothelial cell; PDs, population doublings of cultured cells; CPDL, cumulative population doubling level; SA, senescent-associated; PECAM, platelet/endothelial cell adhesion molecule; m.o.i., multiplicity of infection; BSA, bovine serum albumin; ERK, extracellular signal-regulated kinase; siRNA, small interference RNA; BrdUrd, bromodeoxyuridine; RT, reverse transcription.

chemotaxis and $S1P_2$ inhibits it. Thus, the physiological responses of S1P may be an orchestrated manifestation between the signaling cascades activated by the S1P receptor subtypes.

Most primary human cultures have a finite lifespan *in vitro*. By serial subculture, cells will cease proliferation and enter an irreversible state of terminal differentiation, which is termed replicative senescence. Cellular senescence is thought to be an important tumor-suppressive mechanism *in vivo* (17). For example, it was shown that senescence prevents the replication of neoplastic cells and thus inhibits tumor formation in the young animal. In contrast, the accumulation of senescent cells during the aging process may have detrimental effects. The number of senescent cells increases in the elderly can alter the tissue homeostasis (18). Also, it has been suggested that senescent ECs may be responsible for impaired wound healing and angiogenesis in the elderly (19). Moreover, altered gene expression by senescent ECs can negatively impact the surrounding microenvironment. For example, nitric oxide (NO) is a multifunctional mediator involved in vasodilatation and angiogenesis (20). NO production was shown to be inhibited in senescent ECs (21), suggesting that accumulation of senescent ECs *in vivo* may affect vascular tone and homeostasis. Furthermore, senescent ECs were shown to be present in human atherosclerotic lesions but not in non-atherosclerotic lesions (22, 23). These results together suggest that senescent ECs *in vivo* may contribute to the pathogenesis of human vascular diseases.

Sphingolipids have been shown to play critical roles in mediating cellular senescence and regulating senescent-associated dysfunctions (24–28). In this study, we utilized cultured ECs as an *in vitro* model to investigate the underlying mechanisms of senescent-associated endothelial impairments. We demonstrate that the senescent-associated endothelial dysfunctions can be attributed to the up-regulation of $S1P_2$ signaling. This study is significant because it shows for the first time the functional balance between $S1P_1$ and $S1P_2$ signaling in regulating physiological events such as senescent-dependent impairments of wound-healing and morphogenetic capabilities in vascular ECs.

EXPERIMENTAL PROCEDURES

Reagents—S1P purchased from Biomol was dissolved in 4 mg/ml fatty acid-free BSA (Sigma). Mouse monoclonal $S1P_1$ antibody E1–49 (IgG 2b) (29) was generated by conventional hybridoma technology using bacteria-expressed $S1P_1$ as immunogen. Phospho-specific anti-Akt1 was from Calbiochem, monoclonal mouse anti-Rac was from Upstate, and polyclonal rabbit anti-Akt and polyclonal rabbit phospho-specific anti-ERK1/2 were purchased from Cell Signaling. Polyclonal rabbit anti-ERK2 and anti-actin (H-300) were purchased from Santa Cruz Biotechnology (Santa Cruz, CA). Protein G-ultralink and A-Trisacryl beads were from Pierce. Peroxidase-conjugated sheep anti-rabbit IgG and peroxidase-conjugated goat anti-mouse IgG was from MP Biomedicals and Pierce Biotechnology, respectively. Matrigel was from BD Biosciences. For immunohistochemical staining, polyclonal rabbit anti-$S1P_1$ and anti-$S1P_2$ were provided by Dr. Suzanne Mandala (Merck Research Laboratories). Alexa-conjugated secondary antibodies and an ABC kit were from Molecular Probes and Vector laboratories, respectively. Other reagents, unless specified, were purchased from Sigma.

Cell Culture and Adenoviral Transduction—ECs with different *in vitro* ages were established essentially as described (30). Briefly, human umbilical vein endothelial cells (HUVECs) were plated at 4×10^5 cells in a 100-mm culture dish and split every 3 days. The number of population doublings (PDs) that occurred during each passage was calculated as PD = $\log_2$ (number of cells proliferated/number of cells seeded). The cumulative population doubling level (CPDL), used to represent the age of the ECs *in vitro*, is the sum of PDs of each passage. According to this protocol, HUVECs became senescence at CPDL = 60. Senescence was verified by the expression of senescent-associated (SA) β-galactosidase, a specific biomarker for senescent cells (31), and the lack of BrdUrd nuclear labeling (Zymed Laboratories Inc.), an indicator of cell proliferation. HUVECs of three stages were used throughout this study: young, intermediate, and senescent ECs with CPDLs of 15, 35, and 60, respectively. The transduction of endothelial cells with adenoviral particles was essentially as described before (13, 29).

Electric Cell-substrate Impedance Sensing (ECIS) Assay—The ECIS™ Model 1600R (Applied BioPhysics) was used to measure the endothelial wound-healing responses essentially as described (29, 32). Briefly, 200 μl of cell suspension (5×10^5 cells per ml) was seeded to each well of either an 8W1E or 8W10E ECIS array (Applied BioPhysics), which was pre-equilibrated with 200 μl of medium at 37 °C for 30 min. Two days later, endothelial cells were washed and replaced with plain M199 medium supplemented with 0.5% fetal bovine serum. For assessing wound-healing responses, the cell-covered electrode was connected to an AC source. By applying 5 V for 30 s, a relatively high current is delivered to the cell-covered electrode, which results in cell killing (29, 32). After stimulating without or with S1P, endothelial wound-healing responses were determined in real-time by measuring the recovery of electrical impedance, an indicator of endothelial migration and proliferation into the wounded area (29, 32).

Endothelial Morphogenesis and Rac Activation—The *in vitro* endothelial morphogenesis assay was performed in three-dimensional Matrigel (BD Biosciences) as described (12, 13, 33). Rac activity was measured as described (13). Briefly, HUVECs of different CPDLs were treated without or with S1P for various times. Cells were collected and solubilized with magnesium-containing lysis buffer (25 mM HEPES, pH 7.6, 150 mM NaCl, 1% Nonidet P-40, 10% glycerol, 25 mM NaF, 10 mM $MgCl_2$, and 1 mM EDTA) containing protease inhibitors (Calbiochem). 400 μg of cell extracts was incubated with glutathione *S*-transferase-p21-activated kinase (Rac binding domain of p21-activated kinase) beads at 4 °C for 1 h to isolate the GTP-bound form of activated Rac. After washing, bound Rac polypeptides were resolved on a 12% SDS-PAGE and detected by Western blot analysis with monoclonal Rac antibody.

Immunoprecipitation and Western Blot Analysis—HUVECs treated without and with S1P were collected with cell scrapers in ice-cold phosphate-buffered saline followed by centrifugation (250 × *g*, 5 min). Cell extracts were prepared in TBST/OG buffer (10 mM Tris-HCl, pH 8.0, 0.15 M NaCl, 1% Triton X-100,

60 mM *n*-octyl β-D-glucopyranoside) containing protease inhibitors (Calbiochem) with constant agitation at 4 °C for 30 min, followed by centrifugation at 15,000 × *g* for 20 min. Cell extracts were incubated overnight at 4 °C with the indicated antibodies, and the immunocomplexes were precipitated by adding the mixtures of protein-A and protein-G beads at 4 °C for 1 h. After washing, precipitated polypeptides were released by boiling in double-strength Laemmli buffer at 95 °C for 5 min, resolved on a 10% SDS-PAGE, and transferred to nitrocellulose membranes. Subsequently, the membranes were blocked in 5% nonfat dry milk (Lab Scientific) in TBST (20 mM Tris-HCl, pH 7.4, 500 mM NaCl and 0.1% Tween 20). The blots were washed and incubated with the indicated primary antibodies on a rotary shaker at 4 °C for overnight. The blots were then incubated with horseradish peroxidase-conjugated second antibody for 1 h at room temperature, incubated with enhanced chemilumenescence reagent (ECL) (Amersham Biosciences) for 1 min, and visualized by exposure to Kodak X-Omat films.

PTEN Phosphatase Assay—PTEN phosphatase activity was measured with the PTEN Malachite Green Assay Kit (Upstate) according to the manufacturer's instructions. Endothelial cells with different *in vitro* lifespans were solubilized in a lysis buffer containing 20 mM Tris, 300 mM NaCl, 2 mM EDTA, 0.2% SDS, 2% Triton X-100, and protease inhibitors (Calbiochem). After centrifuging at 15,000 × *g* for 20 min, cellular PTEN polypeptides were immunoprecipitated by incubating extracts (500 μg) with anti-PTEN (Cell Signaling) at 4 °C overnight, followed by adding protein-A beads for 1 h at 4 °C. The precipitated PTEN was then assessed for phosphatase activity by using D-myo-phosphatidylinositol 3,4,5-triphosphate (Echelon Biosciences, Salt Lake City) containing phospholipids vesicles. The released phosphate was quantitated after the addition of the malachite green reagent (Upstate) by measuring the absorbance at 630 nm.

RT-PCR and Real-time PCR—Total RNA was isolated from cultured cells using the RNeasy kit (Qiagen) and was reverse-transcribed with an oligo-dT primer (Invitrogen) by M-MLV Reverse Transcriptase (Promega, Madison, WI) for first strand cDNA synthesis. PCR detection of each gene expression was performed with 2 μl of reverse-transcribed cDNAs in a total volume of 20 μl of reaction mixture containing 200 nM of each primer, 0.2 mM of each dNTP, and 1 unit of *Taq* polymerase (Promega). Reactions were performed using the GeneAmp 9700 PCR System (Applied Biosystems). PCR conditions were performed with 35 cycles of denaturation at 95 °C (30 s), annealing at 58 °C (30 s), and extension at 72 °C (30 s). Amplified PCR products were analyzed by electrophoresis on a 1.5% agarose gel. PCR primer pairs used were: human $S1P_1$: sense, 5′-GCACCAACCCCATCATTTAC-3′, antisense, 5′-TTGTCCCCTTCGTCTTTCTG-3′; human $S1P_2$: sense, 5′-CAAGTTCCACTCGGCAATGT-3′, antisense, 5′-CAGGAGGCTGAAGACAGAGG-3′; human $S1P_3$: sense, 5′-TCAGGGAGGGCAGTATGTTC-3′, antisense, 5′-GAGTAGAGGGGCAGGATGGT-3′; human $S1P_4$: sense, 5′-AGCCTTCTGCCCCTCTACTC-3′, antisense, 5′-ATCAGCACCGTCTTCAGCA-3′; and human $S1P_5$: sense, 5′-ACAACTACACCGGCAAGCTC-3′, antisense, 5′-GCCCCGACAGTAGGATGTT-3′. For real-time PCR quantitation, 50 ng of reversely transcribed cDNAs were amplified with the ABI 7500 system (Applied Biosystems) in the presence of TaqMan DNA polymerase. The sense and antisense primers used to detect the gene expression of S1P receptor subtypes and glyceraldehyde-3-phosphate dehydrogenase were purchased from Applied Biosystems. The qPCR reaction was performed by using a universal PCR Master Mix (Applied Biosystems) according to the manufacturer's instructions.

siRNA-mediated Gene Silencing—To specifically knockdown the endothelial $S1P_2$ receptor, sense and antisense hairpin oligonucleotides flanked with BamH1 and EcoRI restriction sites at 5′- and 3′-ends, respectively, were designed according to GenScript siRNA sequence design tool (siRNA target finder, www.genscript.com/ssl-bin/app/rnai). The oligonucleotide sequences were: (sense), 5′-gatccGTGACCATCTTCTCC-ATCATTCAAGAGATGATGGAGAAGATGGTCACTTTT-TTg-3′; (antisense), 5′-aattcAAAAAAGTGACCATCTTCTC-CATCATCTCTTGAATGATGGAGAAGATGGTCACg-3′. The sense and antisense oligonucleotides were annealed and cloned into lentiviral pFIV-H1 vector (System Bioscience). Lentiviral transducing particles carrying the siRNA oligonucleotides were produced by packaging in the 293T/17 cell line following the manufacturer's instructions. Lentiviral particles carrying siRNA oligonucleotide for luciferase were used as a control. HUVECs (6×10^5 cells) were infected with lentiviral particles (~0.1, multiplicity of infection (m.o.i.)) in 60-mm dishes for 24 h in the presence of polybrene (2 μg/ml), washed, and replaced with fresh medium for an additional 24 h. Subsequently, cells were split (1:3 split ratio), and HUVECs stably transduced with the lentiviral particles were isolated by puromycin (1 μg/ml) selection.

Migration Assay—Endothelial chemotaxis was measured using the Transwell migration assay (8-μm pore size, Costar) as described (13, 29). Briefly, polycarbonate membranes were coated with human fibronectin (1 μg/ml) overnight at 4 °C. Following serum starvation, HUVECs were trypsinized, counted, and resuspended in M199 media with 0.5% fatty-acid free BSA (Sigma). Cells (7.5×10^4 cells in 100 μl) were placed in the upper chamber, and medium (600 μl) containing S1P was added to the lower chamber. ECs were allowed to migrate for 4 h at 37 °C in a humidified chamber with 5% CO_2. Subsequently, the non-migrated cells on the upper side of the filter were removed with a cotton swab. The filters were fixed with 4% formaldehyde and stained with 0.1% crystal violet solution. Following eluting the stained dye with 10% acetic acid, cell chemotaxis was quantitated with the BMG FluoStar Galaxy microplate reader (BMG Labtechnologies) with absorbance at 590 nm.

Immunohistochemical Analysis—Paraffin sections were prepared from aorta of atherosclerotic mice as previously described (34). Subsequently, aortic specimens were blocked with 5% BSA in phosphate-buffered saline and incubated with indicated antibodies (1:100 dilution in 1% BSA) overnight at 4 °C. After washing with phosphate-buffered saline (3 × 5 min), specimens were incubated with biotin-conjugated secondary antibody (1:200 dilution in 1% BSA, Vectastain-Elite-ABC-Kit) for 30 min at room temperature, followed by incubation with avidin-biotinylated horseradish peroxidase solution (Vectastain-Elite-ABC-Kit) for 30 min at room temperature. Immu-

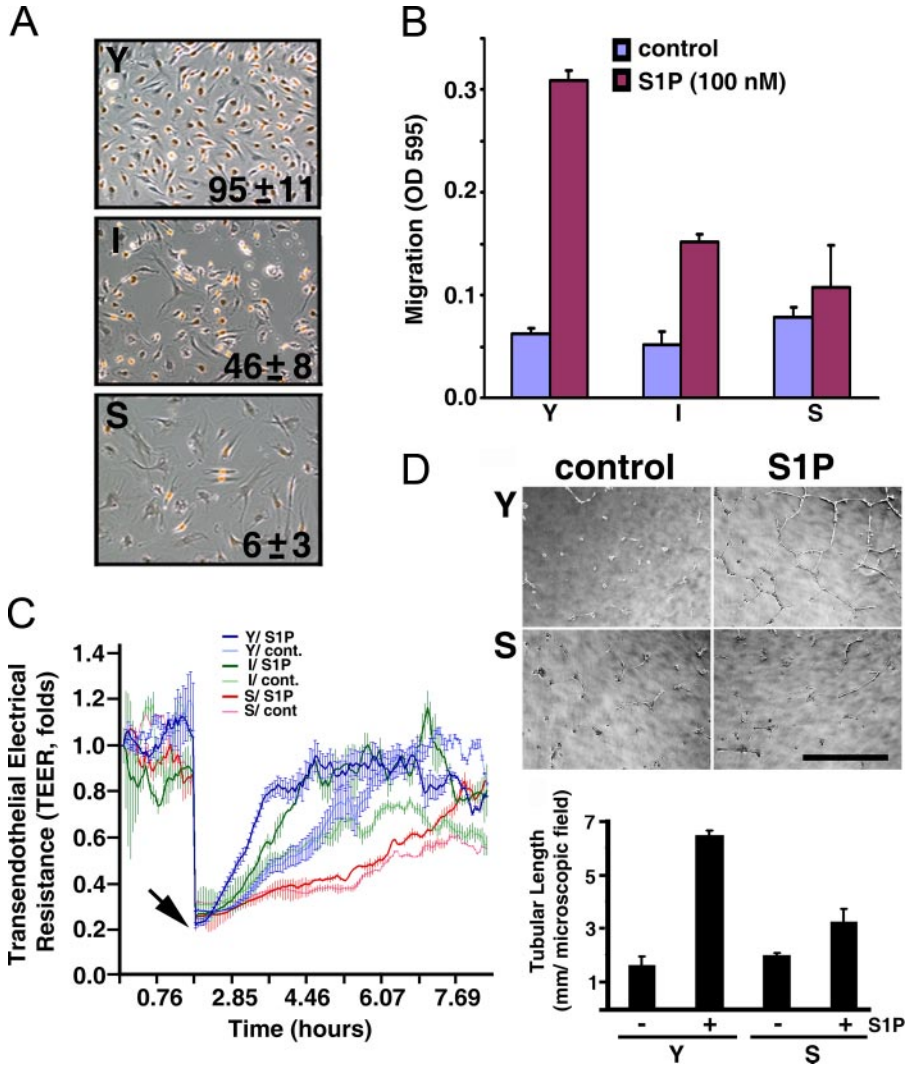

FIGURE 1. **S1P-mediated endothelial functions are impaired in senescent ECs.** *A*, proliferative capabilities of young (*Y*, CPDL = 15), intermediate (*I*, CPDL = 35), and senescent (*S*, CPDL = 60) ECs. Cells were labeled with BrdUrd reagent for 24 h. Subsequently, cells were immunostained with anti-BrdUrd following the manufacturer's instructions (BrdUrd staining kit, Zymed Laboratories Inc.). Mean ± S.E. represents percentage of BrdUrd incorporated nuclei from 3–5 microscopic fields of duplicate experiments. *B*, chemotactic responses were measured by a Transwell migration assay as described under "Experimental Procedures." Note that S1P (100 nM)-induced chemotactic responses were inversely related to *in vitro* ages of cultured ECs. *C*, young, intermediate, and senescent ECs were plated into each well of 8W1E arrays and incubated at 37 °C to allow the transendothelial electrical resistance (TEER) to reach equilibrium. 24 h later, the cells attached to the microelectrodes were killed by applying 5 V of electrical current for 30 s (*arrow*), which resulted in an abrupt impedance drop. Subsequently, endothelial wound-healing responses in the presence or absence of 100 nM S1P were determined in real-time by measuring the recovery of TEER, an indicator of endothelial migration into the wounded area (29). *D*, morphogenesis of young and senescent ECs on matrigel (*upper panel*) and quantitative analysis of tubular length (*lower panel*) in the presence or absence of S1P (200 nM) were performed as described (12, 13). *Scale bar*, 318 μm.

nostaining was then developed by diaminobenzidine tetrachloride solution according to manufacturer's instructions (Vector Laboratories). Specimens were counterstained with hematoxylin solution (Sigma). Because horseradish peroxidase enzymes specifically bound to antigen-antibody complexes were visualized by the addition of diaminobenzidine tetrachloride chromogen, the intensity of brown staining indicates the relative abundance of antigen. For quantitative purposes, the immunoreactivity (*i.e.* the intensity of brown staining) was analyzed by MetaMorph image acquisition and analysis software (MetaMorph Version 6.1, Molecular Devices) (35). In addition, specimens were counterstained with hematoxylin solution, which produces a contrasting purple color for negative cells. The staining of SA-β-galactosidase was performed essentially as described (22, 23, 31).

RESULTS

Impaired Chemotactic, Wound-healing, and Morphogenetic Responses in Senescent ECs—We established HUVECs with different *in vitro* ages by the standard protocol of serial subculture (30). HUVECs reach their *in vitro* lifespan at a CPDL of 60. Endothelial senescence was verified using SA-β-galactosidase staining and BrdUrd labeling (31). SA-β-galactosidase activity, a biomarker for cell senescence, was detected in over 90% of the senescent ECs. Also, BrdUrd labeling, an indicator of cell proliferation, was observed in >95, 46, and 6% of young (CPDL = 15), intermediate (CPDL = 35), and senescent (CPDL = 60) ECs, respectively (Fig. 1*A*).

Next, we utilized the potent chemoattractant S1P (13, 29) to examine the chemotactic capability of young, intermediate, and senescent ECs. As shown in Fig. 1*B*, S1P-mediated chemotactic response is inversely related to the *in vitro* ages of ECs. Moreover, S1P is unable to induce detectable chemotaxis in senescent ECs.

S1P greatly accelerates the wound-healing and injury repair process in ECs (29). Therefore, we utilized the electrical cell-substrate impedance sensing (ECIS) technique (29, 32) to measure the S1P-mediated wound-healing response in ECs with different *in vitro* ages. Young, intermediate, and senescent ECs were plated in the ECIS arrays. Subsequently, ECs attached to the microelectrodes (100 μm in diameter) of arrays were killed by applying a high voltage electrical current (5 V for 30 s; *arrow*, Fig. 1*C*). The efficacy of the elevated electrical current to completely kill ECs attached to the microelectrodes was verified by cell viability staining with ethidium homodimer/calcein acetoxymethyl ester (29, 32) and was shown by the complete drop of transendothelial electrical resistance (TEER) to the basal level (*arrow*, Fig. 1*C*). In contrast, the elevated electrical current had no effect on cells surrounding the microelectrodes (29, 32). These viable cells surrounding the microelectrodes then migrate into electrically wounded areas, proliferate, re-establish the cell-cell interactions, and

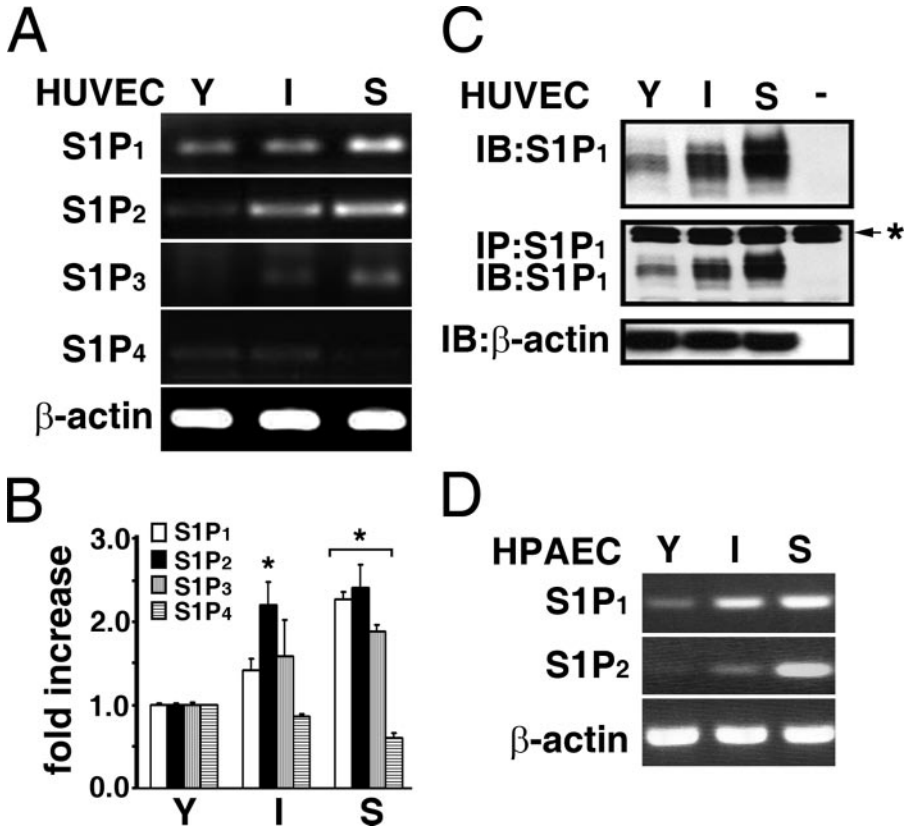

FIGURE 2. **Expression of S1P family receptor subtypes in ECs with different *in vitro* ages.** The expression of S1P receptor subtypes in young, intermediate, and senescent HUVECs was measured by RT-PCR (*A*) and real-time qPCR (*B*) as described under "Experimental Procedures." $S1P_1$ expression was age-dependently increased in cultured HUVECs, and $S1P_2$ expression was barely detected in young ECs, whereas it was markedly increased in intermediate and senescent ECs. Similarly, $S1P_3$ was barely detected in young ECs and significantly up-regulated in senescent ECs. A low level of $S1P_4$ receptor was detected in young and intermediate ECs and is absent in senescent ECs. $S1P_5$ was not detected in ECs with different *in vitro* ages. The data are from a representative experiment, which was repeated six times with identical results. *, $p < 0.01$ (*t* test). *C*, endothelial extracts were immunoblotted (*upper panel*), or immunoprecipitated followed by Western-blotting with anti-$S1P_1$ (*middle panel*). Immunoblotting with anti-β-actin was used as an internal control for loading (*lower panel*). The result is representative of triplicate experiments. −, assays were performed without endothelial extracts; *, immunoglobulin heavy chain used for immunoprecipitation assays. *D*, $S1P_1$ and $S1P_2$ expression in HPAECs with different *in vitro* ages. $S1P_1$ expression was age-dependently increased in HPAECs. Also, $S1P_2$ expression was significantly induced in senescent HPAECs and was undetected in young HPAECs.

thus repair the injuries. The sequential events of the wound-healing process can be monitored in real-time by the increasing TEER. As shown in Fig. 1*C*, S1P significantly accelerated this wound-healing response in the electrically injured endothelial monolayer (*t* test, $p < 0.005$). It required ~2 h for young ECs to repair the wounds in the presence of S1P (*thick blue line*, Fig. 1*C*); whereas it required ~5 h for young ECs to repair in the absence of S1P (*thin blue line*, Fig. 1*C*). Moreover, the wound-healing capability is inversely related to the *in vitro* ages of ECs. For example, it required ~4 h for intermediate ECs to maximally repair the wounded area in the presence of S1P (*thick green line*, Fig. 1*C*). In contrast, ~10 h were required for wound repair with senescent ECs treated with S1P (*thick red line*, Fig. 1*C*).

We next employed a Matrigel morphogenesis assay, a widely used model system to assess *in vitro* angiogenic responses (33), to determine the S1P-mediated endothelial morphogenetic responses in young and senescent ECs. ECs were plated on Matrigel and treated without or with S1P. As shown in Fig. 1*D*, young ECs formed an organized network of tubule-like structures after S1P treatment, whereas the ability of S1P to stimulate morphogenesis was completely diminished in senescent ECs. These data together indicate that senescent ECs are severely impaired in proliferative, chemotactic, wound-healing, and angiogenic responses.

Expression of S1P Family of GPCRs in Senescent ECs—We next determined the expression profiles of the S1P family of GPCRs during the *in vitro* aging process in cultured ECs. By analysis with the semi-quantitative RT-PCR (Fig. 2*A*) and real-time PCR (Fig. 2*B*) techniques, $S1P_1$ expression is shown to be significantly increased in an *in vitro* age-dependent manner in cultured ECs. The increased expression of $S1P_1$ receptor during *in vitro* aging process was further confirmed at the protein level by directly immunoblotting ECs extracts (*top panel*, Fig. 2*C*), or by immunoprecipitating endothelial extracts followed by immunoblotting (*middle panel*, Fig. 2*C*) with a monoclonal $S1P_1$ antibody. The expression of the $S1P_3$ receptor was also increased in senescent ECs (Fig. 2, *A* and *B*). It was shown that $S1P_2$ receptors are barely detected in the early passage of ECs (12). Interestingly, we observed that $S1P_2$ expression was dramatically induced in *in vitro* aged ECs (Fig. 2, *A* and *B*). In contrast, the expression of the $S1P_4$ receptor was slightly decreased in senescent ECs (Fig. 2, *A* and *B*), and $S1P_5$ was not detected in young and senescent ECs (data not shown). Furthermore, the *in vitro* aged-dependent induction of $S1P_1$ and $S1P_2$ receptors was observed in human pulmonary artery endothelial cells (HPAECs, Fig. 2*D*). The *in vitro* lifespan of HPAECs (ATCC, CRL-2598) is approximately CPDL = 45. The expression of $S1P_1$ in young (CPDL = 22), intermediate (CPDL = 30), and senescent (CPDL = 45) HPAECs also increased in an *in vitro* aged-dependent manner (*top panel*, Fig. 2*D*). Moreover, similar to $S1P_2$ expression in HUVECs, $S1P_2$ receptors were undetectable in young HPAECs, whereas $S1P_2$ expression is markedly increased in the intermediate and senescent HPAECs (*middle panel*, Fig. 2*D*).

Up-regulation of $S1P_2$ in Aorta of Atherosclerotic Mice—Senescent ECs have been identified in the vascular endothelium in atherosclerosis (22, 23), an aged-associated vascular disorder. We previously developed a mouse model to elucidate the role of leukotriene B4 in atherosclerosis (34). Aorta containing atherosclerotic lesion and non-lesion regions were therefore used to examine the expression of the S1P receptor subtypes *in situ* (Fig. 3). The endothelial layers were identified by immuno-

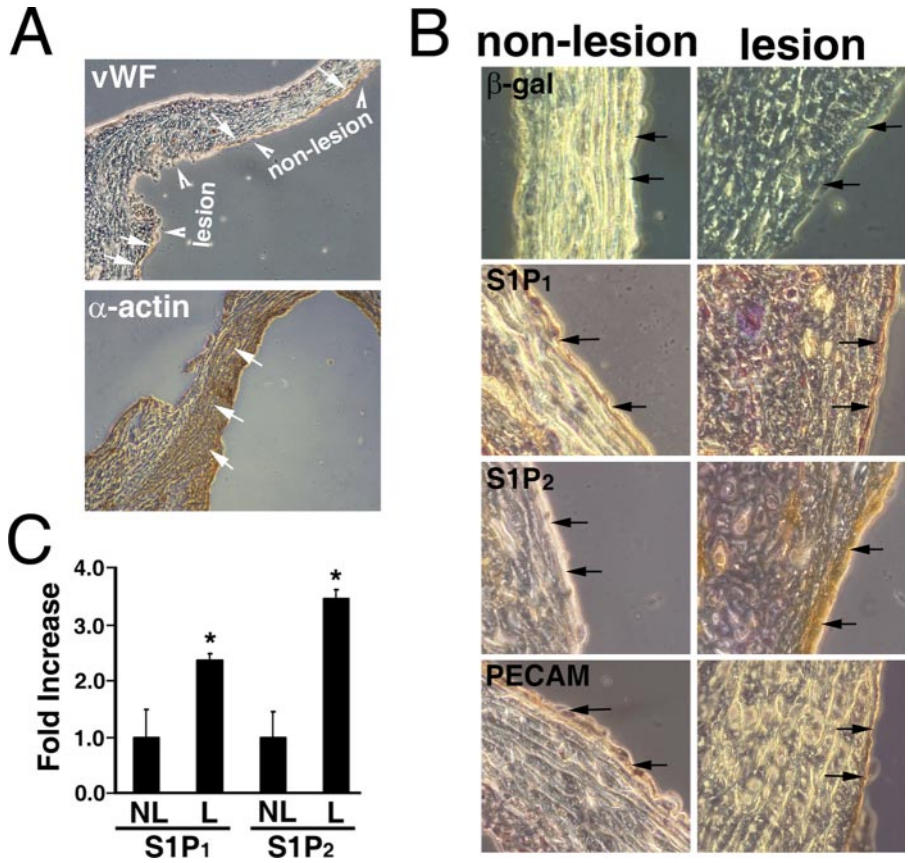

FIGURE 3. **$S1P_2$ receptors are up-regulated in the endothelium at the atherosclerotic lesion.** The aorta segments were prepared from atherosclerotic mice (~25 weeks old) as described previously (34). The atherosclerotic lesion and non-lesion regions (*arrowheads*, *top*, *panel A*) of the aorta were identified as reported previously (34). The endothelium was identified by staining with anti-Von Willebrand factor (*vWF*, *arrows*, *top*, *panel A*) and anti-PECAM (*arrows*, *bottom row*, *panel B*). The smooth muscle layers were identified by anti-α-actin staining (*arrows*, *bottom*, *panel A*). *B*, the non-lesion and lesion regions of atherosclerotic aorta were examined for expression of SA-β-galactosidase activity (*top row*), $S1P_1$ (*second row*), and $S1P_2$ (*third row*). SA-β-galactosidase activity was observed in the endothelium of lesion regions (*blue color* indicated by *arrows*) and absent in the non-lesion regions. A small increase of $S1P_1$ expression was observed in lesion regions compared with the non-lesion regions (*brown color* indicated by *arrows*, *second row*). The expression of $S1P_2$ receptors was not detected in the endothelium of the non-lesion regions of the aorta (*light brown* indicated by *arrows*, *left panel*, *third row*). In contrast, $S1P_2$ receptors were markedly up-regulated in the endothelium of atherosclerotic lesions (*dark brown* indicated by *arrows*, *right panel*, *third row*). *C*, quantitation of $S1P_1$ and $S1P_2$ expression. The expression of $S1P_1$ and $S1P_2$ receptors in lesion and non-lesion regions of the atherosclerotic endothelium was quantitated by MetaMorph software (MetaMorph Version 6.1, Molecular Devices) (35). Data represent mean ± S.E. of six microscopic fields. Both $S1P_1$ and $S1P_2$ receptors are significantly up-regulated in the lesion regions of atherosclerotic endothelium (*, $p < 0.05$, *t* test). *NL*, non-lesion; *L*, lesion regions.

staining with antibodies to Von Willebrand factor (indicated by *arrows*, *top panel*, Fig. 3*A*) and PECAM (*arrows*, *bottom row*, Fig. 3*B*). The smooth muscle layers were characterized by immunostaining with α-actin antibodies (*arrows*, *bottom panel*, Fig. 3*A*). In agreement with previous reports (22, 23), SA-β-galactosidase-positive ECs (*i.e.* senescent ECs) were clearly identified in the endothelial layer of the atherosclerotic lesion (*dark blue layer* indicated by *arrows*, *top right panel*, Fig. 3*B*). In contrast, no senescent ECs were identified in the non-lesion region of the aortic endothelium (*light blue cell layer* indicated by *arrows*, *top left panel*, Fig. 3*B*).

We next examined the expression of $S1P_1$ and $S1P_2$ receptors in the lesion and non-lesion regions of atherosclerotic aorta by immunohistochemical staining followed by quantitation with MetaMorph image acquisition and analysis software. The immunohistochemical staining was developed by the diaminobenzidine tetrachloride reagent and counterstained with hematoxylin. Therefore, the intensity of brown staining quantitatively indicates the expression of $S1P_1$ or $S1P_2$ receptors, and the negative cells that were counterstained with hematoxylin show purple staining. As shown in Fig. 3*B*, the immunoreactivity of the $S1P_1$ antibody was increased in the endothelial layer of the atherosclerotic lesion (*light brown versus dark brown* in non-lesion *versus* lesion, *arrows*, *second row*, Fig. 3*B*). Indeed, quantitative analysis shows that there is a 2.4 ± 0.1-fold increase ($n = 6$, $p < 0.05$, *t* test) of $S1P_1$ receptors in the lesion region of atherosclerotic aorta (Fig. 3*C*). Importantly, $S1P_2$ was barely detectable in the non-lesion endothelium (*light brown*, *arrows*, *left panel*, *third row*, Fig. 3*B*). In sharp contrast, $S1P_2$ expression was dramatically increased in the endothelium of the atherosclerotic lesion (*dark brown*, *arrows*, *right panel*, *third row*, Fig. 3*B*). Quantitative analysis shows that there is a 3.5 ± 0.2-fold increase ($n = 6$, $p < 0.05$, *t* test) of $S1P_2$ receptors in the lesion region of atherosclerotic aorta (Fig. 3*C*). Together, these data indicate that the up-regulation of the $S1P_1$ and $S1P_2$ receptors in senescent ECs is physiologically significant.

Elevated PTEN Activity and Diminished Rac Activation in Senescent ECs—Next, we investigated the underlying mechanisms of the functional impairments in senescent ECs. It was previously shown that S1P signaling via $S1P_1/S1P_3$ receptors activates Akt and ERK1/2 (12, 13). Thus, young, intermediate, and senescent ECs were serum-starved, and S1P-induced Akt and ERK1/2 activation was measured by immunoblotting with phospho-specific antibodies. As shown in Fig. 4*A*, S1P effectively activated Akt in young, intermediate, and senescent ECs with approximately similar kinetics. A robust Akt activation was observed 5 min after S1P stimulation, and S1P-induced Akt activation was sustained for up to 1 h in ECs with different *in vitro* ages. Similarly, S1P also activated ERK1/2 in senescent ECs with comparable kinetics as observed in young and intermediate ECs (Fig. 4*B*). Furthermore, there was no significant difference in the quantity of endogenous Akt and ERK1/2 protein between young, intermediate, and senescent ECs (Fig. 4, *A* and *B*). These data show that S1P-mediated ERK1/2 and Akt signaling cascades remain fully functional in senescent ECs.

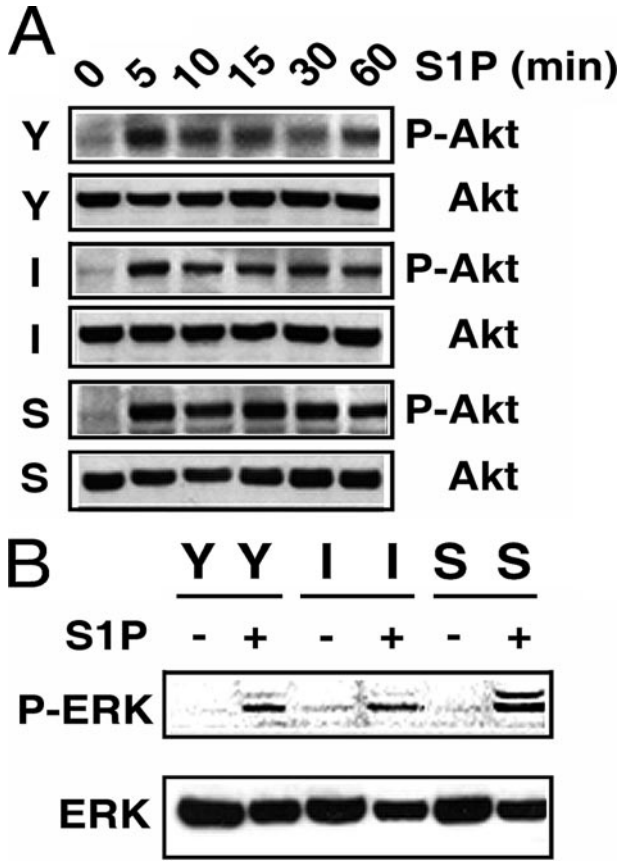

FIGURE 4. **Akt and ERK1/2 are effectively activated in senescent ECs.** Young (*Y*), intermediate (*I*), and senescent (*S*) ECs (8×10^5 cells in 100-mm dish) were plated for 3 days. Cells were then serum-starved in plain M199 medium for 2 h followed by stimulation with S1P (200 nM) for various times. Extracts were then probed with phospho-specific Akt (*panel A*) or phospho-specific ERK (*panel B*) antibody. Subsequently, nitrocellulose membranes were stripped and re-probed with anti-Akt (*panel A*) or anti-ERK (*panel B*) to detect the quantities of endogenous Akt or ERK polypeptides. The experiment was repeated three times with identical results.

Subsequently, we assayed Rac activity in normally growing young, intermediate, and senescent ECs. As shown in Fig. 5*A*, ECs with different *in vitro* ages expressed similar amounts of Rac polypeptides. However, Rac activity was significantly diminished in intermediate ECs, and barely detectable in senescent ECs (*top panel*, Fig. 5*A*). Moreover, S1P-stimulated Rac activation was inversely related to the *in vitro* ages of ECs (*lower panel*, Fig. 5*A*). Recently, it was shown that PTEN (phosphatase and tensin homolog deleted on chromosome 10) negatively regulates Rac activation and cell migration (16). Indeed, PTEN activity was markedly elevated in senescent ECs (Fig. 5*B*). The assay for PTEN activity is specific because the transduction of adenoviral particles carrying the dominant-negative PTEN construct (PTEN-C/S, the catalytic Cys-124 is mutated to Ser) (36) significantly abrogated PTEN activity; whereas transduction of adenoviral particles carrying wild-type PTEN construct had no effect (Fig. 5*B*). Furthermore, when serum-starved young and senescent ECs were stimulated with S1P, PTEN was significant activated in senescent ECs (Fig. 5*C*). These data suggest that the elevated PTEN activity and reduced Rac activation may be the major factor contributing to the impaired functions in senescent ECs.

Impaired Functions in Senescent ECs Are Revoked by the Inhibition of S1P$_2$/PTEN Signaling—We next examined whether the elevated S1P$_2$ signaling results in impairment of S1P-mediated responses in senescent ECs. As shown in Fig. 6*A*, transduction with lentiviral particles carrying si-S1P$_2$ specifically knocked down >95% of S1P$_2$ expression in senescent ECs, whereas transduction with lentiviral particles carrying control siRNA of an irrelevant gene (Luciferase) had no effect. The lentiviral-mediated S1P$_2$ knockdown is specific, because both S1P$_1$ and actin remain intact in si-S1P$_2$-transduced ECs (*two lower panels*, Fig. 6*A*). Moreover, S1P$_2$ knockdown resulted in a significant increase in Rac activity in S1P-stimulated senescent ECs (-fold increase, 5.6 ± 0.4 *versus* 1.9 ± 0.6 in si-S1P$_2$ *versus* si-Luc transduced cells, respectively, $n = 3$) (Fig. 6*B*). In addition, S1P$_2$ knockdown markedly reinstated S1P-induced chemotactic responses in senescent ECs, comparable to that in young ECs (Fig. 6*C*). It should be noted that there is a small but marked increase of Rac activity (Fig. 6*B*, -fold increase, 2.1 ± 0.3 *versus* 1.1 ± 0.5 in si-S1P$_2$ *versus* si-Luc transduced ECs, without S1P addition, $n = 3$) and chemotactic response (Fig. 6*C*, $A_{595\ nm}$, 0.149 ± 0.009 *versus* 0.068 ± 0.013 in si-S1P$_2$ *versus* si-Luc transduced ECs, without S1P addition, $n = 3$) in si-S1P$_2$ knockdown ECs without S1P stimulation. This small increase in Rac activation and migratory response in S1P$_2$ knockdown ECs may be due to the relief of senescent ECs from the constraint of S1P$_2$ inhibitory signaling. Finally, S1P-stimulated wound-healing capability was markedly restored in senescent ECs transduced with si-S1P$_2$, whereas there was no detectable restoration in senescent ECs transduced si-Luc (Fig. 6*D*).

Subsequently, we determined whether S1P-mediated endothelial responses could be restored in senescent ECs by inhibiting PTEN activity. Senescent ECs were transduced with adenoviral particles carrying wild-type or dominant negative PTEN mutant vector, and the Rac activity was measured after stimulating without or with S1P. S1P treatment resulted in a dramatic increase of Rac activation in senescent ECs transduced with adenoviral particles carrying the DN-PTEN vector (Fig. 7*A*). In contrast, senescent ECs transduced with adenoviral particles carrying wild-type PTEN were unable to further augment the S1P-induced Rac activation. Moreover, the inhibition of endogenous PTEN by the expression of the DN-PTEN mutant restored S1P-mediated chemotactic (Fig. 7*B*) and wound-healing responses (Fig. 7*C*) in a dose-dependent manner. In control experiments, adenoviral particles carrying control vectors (β-galactosidase and WT-PTEN) did not restore the impaired functions to senescent ECs. Furthermore, the impairment of S1P-mediated morphogenesis in senescent ECs was reinstated in a dose-dependent manner by the expression of dominant-negative PTEN polypeptides (Fig. 7*D*).

We recently showed that S1P signaling via the S1P$_1$ receptor induces the ligation of integrin α_v and β_3 subunits and the association of focal adhesion kinase (FAK) and α-actinin with integrin $\alpha_v\beta_3$. This ultimately results in the activation of integrin $\alpha_v\beta_3$ in young ECs (37). However, S1P was unable to induce the activation of integrin $\alpha_v\beta_3$ in senescent ECs (Fig. 8 and supplemental Fig. S1). Thus, we examined whether senescent-elevated PTEN signaling antagonizes S1P$_1$-mediated integrin $\alpha_v\beta_3$ activation in senescent ECs. Confocal microscopic analy-

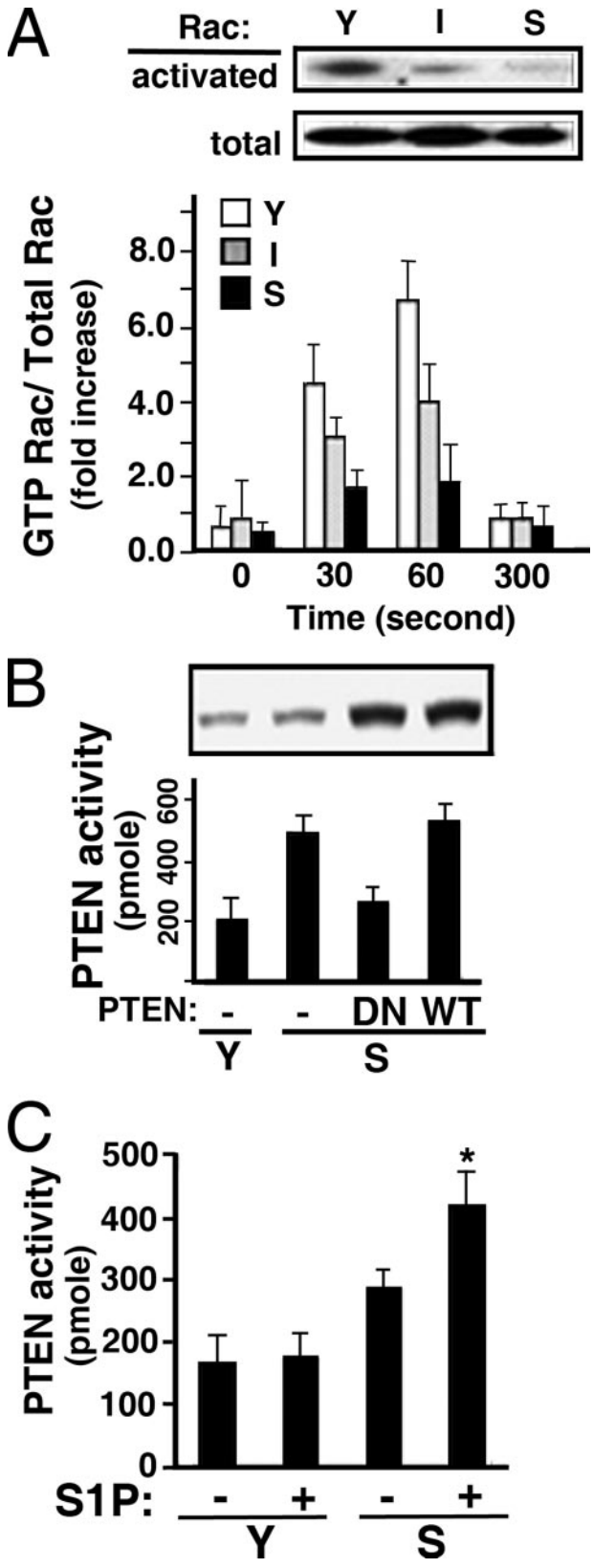

FIGURE 5. **Elevated PTEN and diminished Rac activities in senescent ECs.** *A*: *Upper panel*, cellular lysates were prepared from normally growing young (*Y*), intermediate (*I*), and senescent (*S*) ECs. The activated Rac polypeptides were isolated by glutathione *S*-transferase-p21-activated kinase-bound Sepharose beads as described under "Experimental Procedures" (*upper blot*). Western blots of the cellular extracts (50 μg) with anti-Rac shows that the quantities of endogenous Rac polypeptides were not changed in ECs with different *in vitro* ages (*lower blot*). *Lower panel*, young, intermediate, and senescent ECs were plated for 3 days followed by serum starvation in plain M199. After stimulating with S1P (100 nM) for the indicated times, Rac activation was measured as described above. The immunoblot intensity was quantitated with a Typhoon densitometer equipped with ImageQuant software. The histogram shows S1P-stimulated Rac activation represented as the ratio of activated Rac/total cellular Rac (mean ± S.E., $n = 3$). *B*, cellular extracts of normal growing young and senescent ECs were immunoprecipitated with anti-PTEN. The phosphatase activity of precipitated PTEN was then measured as described under "Experimental Procedures." Alternatively, senescent ECs were transduced with adenoviral particles carrying dominant-negative or wild-type PTEN (200 m.o.i.) for 16 h. The PTEN activity was then measured. *Inset*, Western blot shows the endogenous or transduced PTEN polypeptides. The data are the mean ± S.E. of triplicate determinants. *C*, young and senescent ECs were plated for 3 days followed by serum starvation in plain M199. After stimulating with S1P (100 nM, 15 min), PTEN activity was measured as described above. The data represents the mean ± S.E. of triplicate determinants (*, *t test*; $p < 0.01$).

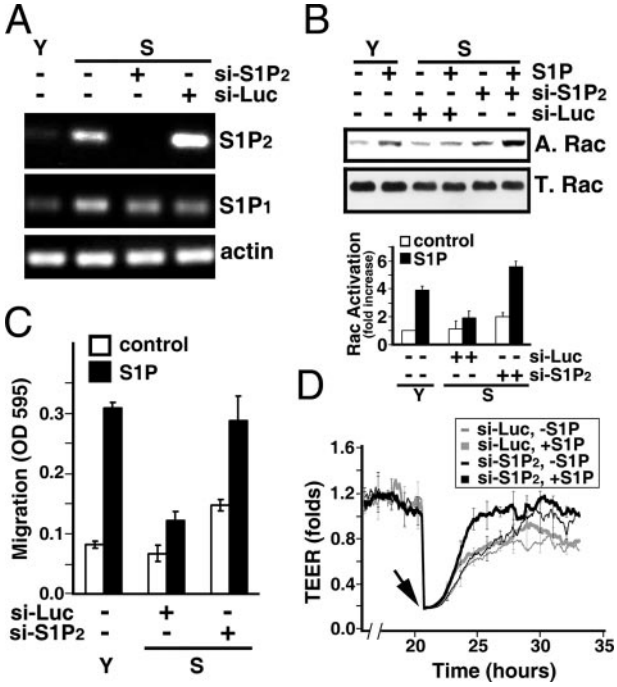

FIGURE 6. **$S1P_2$ knockdown restores the impaired activities of senescent ECs.** *A*, senescent ECs were transduced with lentiviral particles carrying siRNA oligonucleotides for Luciferase or $S1P_2$ receptor. RT-PCR measurement shows the efficacy of $S1P_2$ knockdown. Note that the expression of $S1P_2$ in senescent ECs transduced with a si-$S1P_2$ construct was completely inhibited, whereas an irrelevant siRNA (*si-Luc*) had no effect on $S1P_2$ knockdown. Also note that transduction of si-$S1P_2$ has no nonspecific off-target effects on the expression of $S1P_1$ and actin. *B*, senescent ECs were transduced with lentiviral particles carrying si-$S1P_2$ or si-Luc. Cells were grown for 3 days and serum-starved in plain M199 for 2 h. Subsequently, cells were stimulated with 200 nM S1P for 1 min, and Rac activity was measured as described above. *Fold increase*, mean ± S.E. of three determinants. *C*, endothelial migration was measured in young, si-$S1P_2$-transduced, or si-Luc-transduced senescent ECs in the presence or absence of S1P (100 nM) stimulation. The data are mean ± S.E. of three determinants. *D*, si-$S1P_2$- or si-Luc-transduced senescent ECs were plated in the ECIS array. S1P-mediated wound-healing response was measured as described above. *Arrow*, S1P (200 nM) was added immediately after the endothelial monolayers were injured by elevated electrical voltage. Data are the mean ± S.E. of triplicate determinants of a representative experiment, which was repeated three times with identical results.

sis showed that transduction of dominant-negative PTEN adenoviral particles induced association of FAK and integrin $\alpha_v\beta_3$ at focal adhesion sites in S1P-treated senescent ECs (supplemental Fig. S1). In contrast, transduction of adenoviral par-

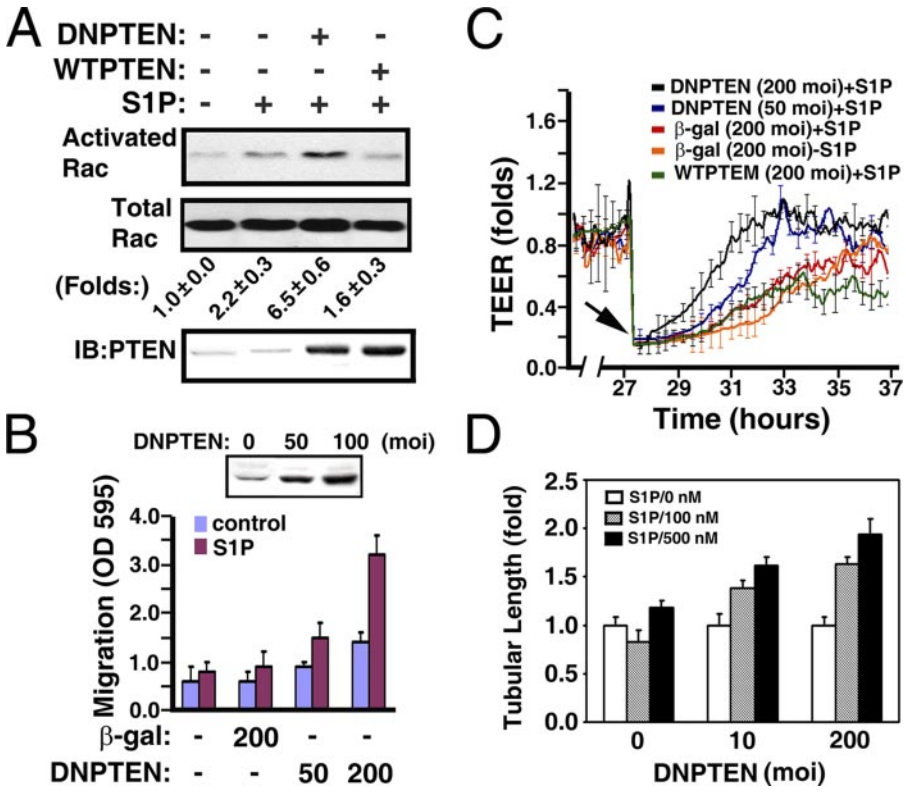

FIGURE 7. **The impaired activities of senescent ECs were restored by dominant negative PTEN.** *A*, senescent ECs (CPDL = 60) were transduced with adenoviral particles (200 m.o.i.) carrying wild-type (*WTPTEN*) or dominant negative PTEN (*DNPTEN*) vectors for 16 h. After S1P stimulation (200 nM, 1 min), Rac activation was measured as described above. *Folds*, mean ± S.E. of three determinants. *Lower panel*, Western blot of cellular extracts shows the expression of endogenous or transduced PTEN polypeptides. *B*, senescent ECs were transduced with adenoviral particles carrying β-galactosidase or DNPTEN vectors for 16 h. Subsequently, the chemotactic responses were measured by Transwell migration assay in the presence or absence of S1P (200 nM). *Inset*, Western blot of cellular extracts shows the expression of transduced dominant negative PTEN polypeptides. The data shows the mean ± S.E. of three determinants. *C*, senescent ECs were grown to confluence in the ECIS array. Cells were then transduced with adenoviral particles carrying β-galactosidase, WTPTEN, and DNPTEN vectors for 16 h. After creating the wound by elevating voltage (*arrow*), S1P-mediated wound-healing responses were monitored in real-time by the increase of TEER. *D*, senescent ECs were infected with adenoviral particles carrying β-galactosidase or DNPTEN vectors. Cells were plated onto three-dimensional Matrigel for 24 h in the presence or absence of the indicated concentrations of S1P. The tubular lengths were quantitated and shown as mean ± S.E. of 3–5 microscopic fields of a representative experiment, which was repeated three times with similar results.

ticles carrying control vector or wild-type PTEN was unable to induce association of FAK with integrin $\alpha_v\beta_3$ at focal adhesion sites in S1P-stimulated senescent ECs (supplemental Fig. S1). Inhibition of PTEN and the resulting integrin $\alpha_v\beta_3$ activation after S1P treatment in senescent ECs were further confirmed by Western blot analysis (Fig. 8). Senescent ECs were transduced with adenoviral particles carrying control, wild-type, or dominant-negative PTEN vectors followed by stimulation without or with S1P. Cellular extracts were immunoprecipitated with LM609, an antibody that immunoreacts with activated integrin $\alpha_v\beta_3$ heterodimers, followed by immunoblotting. As shown in Fig. 8, transduction with dominant-negative PTEN markedly induces association of FAK with integrin $\alpha_v\beta_3$ and ligation of α_v and β_3 subunits. In agreement with our confocal analysis, transduction of adenoviral particles carrying control and wild-type PTEN vectors had no effect on integrin $\alpha_v\beta_3$ activation (Fig. 8). These data indicate that inhibition of integrin $\alpha_v\beta_3$ activation is a downstream effect of PTEN signaling in senescent ECs.

Expression of $S1P_2$ Receptor Inhibits Migration, Wound Healing, and Morphogenesis in Young ECs—To further verify that up-regulation of $S1P_2$ signaling contributes to the SA impairment of endothelial function, we examined whether the expression of $S1P_2$ in young ECs was able to replicate the impairment that occurred in senescent ECs. Young ECs were transduced with various concentrations of adenoviral particles carrying $S1P_2$ receptor. As shown in Fig. 9*A*, young ECs transduced with 100 m.o.i. of adenoviral particles carrying the $S1P_2$ vector ectopically express $S1P_2$ receptors to a level similar to that attained by *in vitro* senescent ECs. Subsequently, young ECs were transduced with adenoviral particles carrying β-galactosidase, $S1P_1$, or $S1P_2$ vectors, and activation of integrin $\alpha_v\beta_3$ at cell migratory edges after S1P stimulation was examined by confocal microscopy. Integrin $\alpha_v\beta_3$ heterodimers were markedly activated in young ECs transduced with adenoviral particles carrying control β-galactosidase or $S1P_1$ receptors (*arrows*, *top two panels*, Fig. 9*B*). There were 92 ± 6% and 87 ± 11% of cells positive for integrin $\alpha_v\beta_3$ activation in young ECs transduced with β-galactosidase and $S1P_1$ adenoviral particles, respectively. In contrast, S1P treatment was unable to activate integrin $\alpha_v\beta_3$ in 72 ± 12% of $S1P_2$ transduced young ECs (Fig. 9*B*). Furthermore, young ECs were co-transduced with adenoviral particles carrying $S1P_2$ and wild-type, or dominant-negative PTEN vectors followed by stimulation without or with S1P. As shown in Fig. 9*C*, co-transduction with dominant-negative PTEN markedly induces the association of α-actinin with integrin $\alpha_v\beta_3$ and the activation of integrin $\alpha_v\beta_3$ in $S1P_2$-transduced young ECs (*arrows*, *bottom row*, Fig. 9*C*). Co-transduction of adenoviral particles carrying wild-type PTEN vectors had no effect on the activation of integrin $\alpha_v\beta_3$ in $S1P_2$-transduced young EC (Fig. 9*C*). Quantitative analysis showed that S1P stimulation resulted in 67 ± 12% (n = 6) of $S1P_2$ and dominant-negative PTEN co-transduced cells exhibiting integrin $\alpha_v\beta_3$ activation and α-actinin-$\alpha_v\beta_3$ association. In contrast, 23 ± 9% (n = 6) of $S1P_2$ and wild-type PTEN co-transduced cells showed integrin $\alpha_v\beta_3$ activation and α-actinin-$\alpha_v\beta_3$ association after S1P treatment.

Moreover, S1P-mediated endothelial migration (Fig. 10*A*) and wound-healing responses (Fig. 10*B*) were inhibited in a dose-dependent manner by the expression of $S1P_2$ receptors in

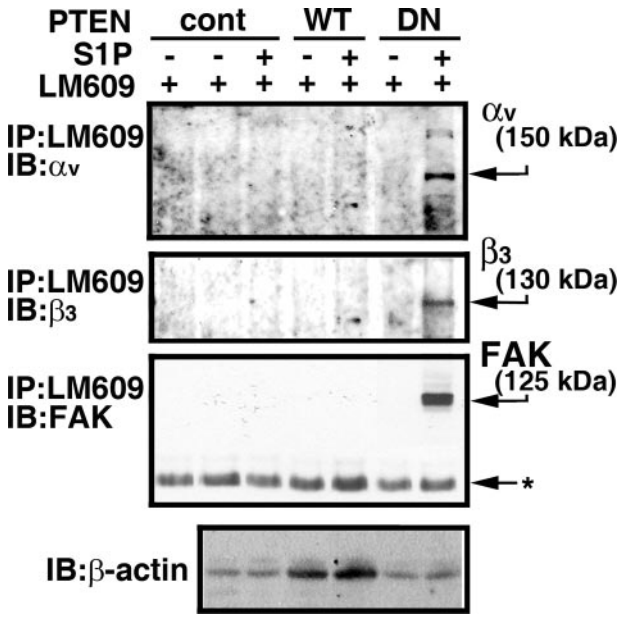

FIGURE 8. **Transduction of dominant-negative PTEN restores S1P-stimulated integrin $\alpha_v\beta_3$ activation in senescent ECs.** Senescent ECs were transduced with adenoviral particles carrying empty vector (*cont*), wild-type (*WT*), or dominant-negative (*DN*) PTEN constructs (200 m.o.i each) for 16 h. Cells were washed and serum starved for 2 h. Subsequently, cells were stimulated with or without S1P (500 nM) for 10 min. Cellular extracts (500 μg) were precipitated with LM609 antibody followed by immunoblotting with FAK, α_v, and β_3 antibodies. The migratory positions of endogenous polypeptides are indicated by *arrows*. Extracts (10 μg) were immunoblotted with β-actin antibody in a parallel assay to show that an equal quantity of extracts was used for the immunoprecipitation assay. *Left lane*, TBST/OG buffer was incubated with LM609 antibody. Note that S1P treatment was unable to induce the association of FAK with integrin $\alpha_v\beta_3$ as well as the ligation of α_v and β_3 subunits in the control vector and wild-type PTEN-transduced senescent ECs. In contrast, S1P stimulated the association of FAK with integrin $\alpha_v\beta_3$ as well as the ligation of α_v and β_3 subunits in dominant-negative PTEN-transduced senescent ECs. The data shown are from a representative experiment, which was repeated two times with similar results.

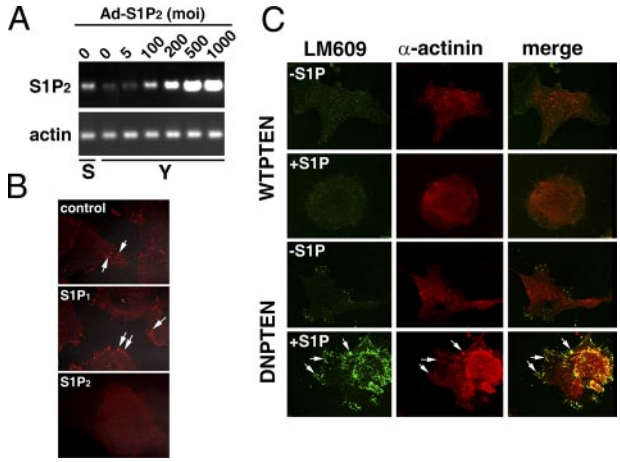

FIGURE 9. **Ectopical expression of $S1P_2$ inhibits integrin $\alpha_v\beta_3$ activation in young ECs.** *A*, young ECs were transduced with increased concentrations of adenoviral particles carrying $S1P_2$ receptors. The expression of $S1P_2$ receptors in senescent (*S*) or young (*Y*) ECs was determined by RT-PCR. Note that the expression of $S1P_2$ receptors in senescent ECs was attained in young ECs by transduction with ~100 m.o.i. of adenoviral particles. *B*, young ECs were transduced with adenoviral particles (100 m.o.i.) carrying the β-galactosidase (*top panel*), $S1P_1$ (*middle panel*), or $S1P_2$ vectors (*bottom panel*). Cells were serum-starved, stimulated with S1P (200 nM, 37 °C for 10 min), and immunostained with mouse monoclonal LM609 (Chemicon). Note that S1P induced the activation of integrin $\alpha_v\beta_3$ at the focal contact sites of the migratory fronts in young ECs transduced with β-galactosidase and $S1P_1$ (*arrows*, *top two panels*). In contrast, S1P was unable to activate integrin $\alpha_v\beta_3$ in young ECs transduced with adenoviral particles carrying $S1P_2$ receptor. *C*, young ECs were co-transduced with adenoviral particles (100 m.o.i. each) carrying $S1P_2$ and wild-type (*first* and *second rows*), or $S1P_2$ and dominant-negative PTEN (*third* and *forth rows*) for 16 h. After stimulation with (*second* and *fourth rows*) or without (*first* and *third rows*) S1P (200 nM, 37 °C for 10 min), cells were immunostained with mouse monoclonal anti-LM609 (*left panels*) and rabbit polyclonal anti-α-actinin (*middle panels*). The *merged images* are shown in the *right panels*. Note that transduction of dominant-negative PTEN induced the co-localization of α-actinin and integrin $\alpha_v\beta_3$ in young ECs expressing $S1P_2$ receptors (*arrows*, *bottom row*). In contrast, S1P treatment was unable to induce integrin $\alpha_v\beta_3$ activation and α-actinin-$\alpha_v\beta_3$ association in young ECs co-transduced with adenoviral particles carrying $S1P_2$ and wild-type PTEN vectors.

young ECs. In contrast, transduction with adenoviral particles carrying the control β-galactosidase vector had no effect on S1P-induced migration (Fig. 10*A*) or wound-healing responses (Fig. 10*B*). Furthermore, the S1P-stimulated formation of a tubular-like network in Matrigel was diminished by the expression of $S1P_2$ receptors in a dose-dependent manner (Fig. 10*C*). Trypan blue exclusion showed that >95% of $S1P_2$-transduced cells were viable, indicating that the inhibition of endothelial functions by $S1P_2$ expression did not result from nonspecific cytotoxic effects (data not shown). These results support the notion that $S1P_2$ signaling negatively regulates chemotactic, wound-healing, and morphogenetic responses in senescent ECs.

DISCUSSION

Research carried out over the past decades has shown that cellular senescence occurs in animals and in other organ systems (19, 22, 23, 38–42). Also, senescent ECs have been identified in vasculature *in vivo* (19, 22, 23). Moreover, the senescent ECs were observed to be present only in lesions of atherosclerotic aorta and not in the normal regions (Fig. 3) (22, 23). This observation implies that endothelial senescence *in vivo* may contribute to the pathogenesis of human atherosclerosis. In the present study, we utilized *in vitro* replicatively senescent ECs to investigate the mechanisms of functional impairments, which might have physiological implications in vascular disorders. An accumulating body of evidence suggests that sphingolipids may play an important role in regulation of cellular senescence (43–47). For example, the intracellular concentration of ceramide was significantly elevated in senescent fibroblasts compared with their young counterparts (43). Also, ceramide was shown to inhibit Cdk2 kinase, increase Kip1 and Kip2 Cdk inhibitors (44), induce dephosphorylation of retinoblastoma tumor suppressor protein (43), inhibit cell growth (45), and induce cellular senescence (43, 46). Moreover, ceramide has been implicated in the inhibition of telomerase activity in human cell lines by inhibiting transcription of the human telomerase gene *hTERT* (47). All of these studies strongly suggest that sphingolipids, particular ceramide, play an important role in regulating pathways related to cellular senescence. S1P, a serum-borne bioactive sphingolipid, regulates various biological activities both *in vitro* and *in vivo*. For example, it has been shown that S1P is an important modulator of endothelial functions, including proliferation, survival, cytoskeletal architecture, chemotaxis, wound-healing, morphogenetic, and angiogenic responses (1–4, 13, 29). However, the role of S1P and its signaling pathways in regulating vascular EC senescence has not been elucidated. Therefore, in the present study, we examined the

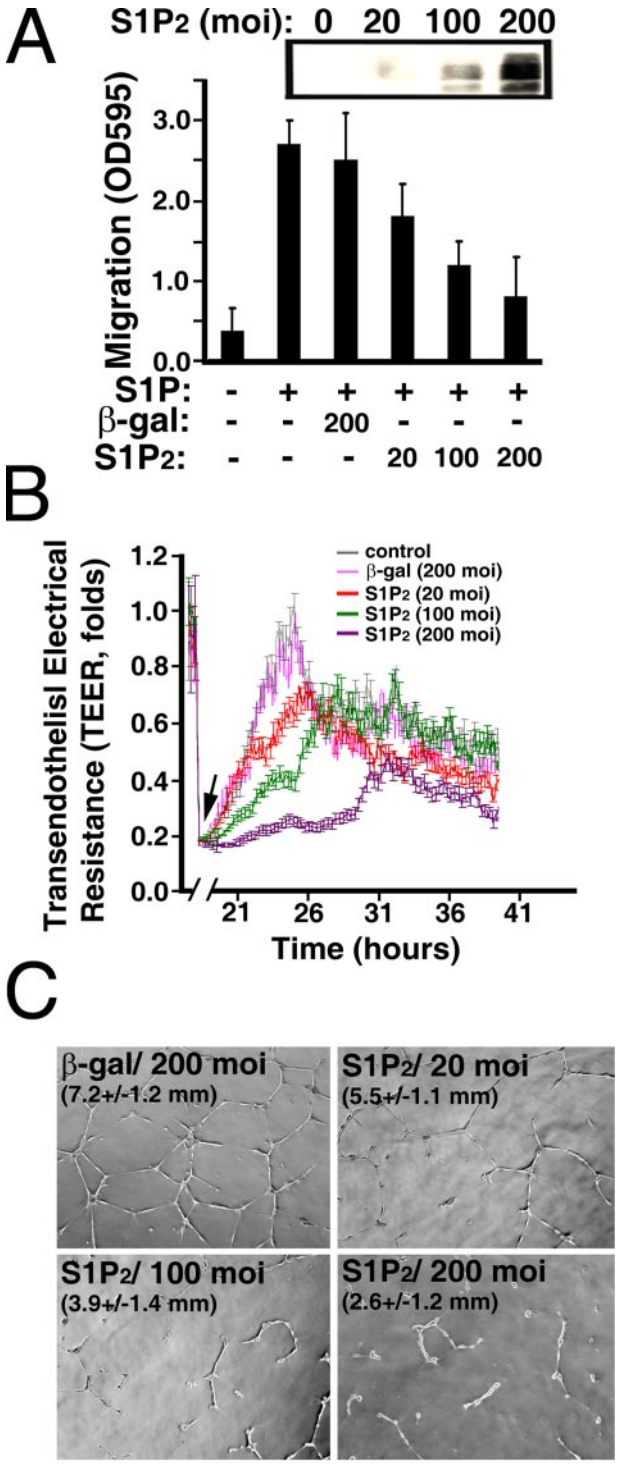

FIGURE 10. **$S1P_2$ expression impairs migratory, wound-healing, and morphogenetic responses in young ECs.** *A*, young ECs (CPDL = 15) were transduced with adenoviral particles carrying β-galactosidase or $S1P_2$ vectors for 16 h. Subsequently, chemotactic responses were measured by a Transwell migration assay in the presence or absence of S1P (200 nM). *Inset*, Western blot of cellular extracts shows the expression of transduced $S1P_2$ polypeptides. *B*, young ECs were grown to confluence in the ECIS array. Subsequently, cells were transduced with adenoviral particles carrying β-galactosidase or $S1P_2$ vectors for 16 h. After creating the wound by elevating voltage (*arrow*), S1P-mediated wound-healing responses were monitored in real-time by the increase of TEER. *C*, young ECs were infected with adenoviral particles carrying β-galactosidase or $S1P_2$ vectors. Cells were plated onto growth factor-reduced Matrigel for 24 h in the presence of S1P (200 nM). The tubular lengths were quantitated as described (12, 13). Magnification, ×5. The data in *A*, *B*, and *C* are mean ± S.E. of three determinants of a representative experiment, which was repeated at least three times with similar results.

response of cultured ECs of different *in vitro* ages to S1P stimulation. We observed that S1P-mediated chemotactic, wound-healing, and morphogenetic responses were inversely related to the *in vitro* age of cultured ECs (Fig. 1). Cultured ECs at early passage abundantly express $S1P_1$ receptors and few $S1P_3$ receptors (12). The SA functional impairments were not due to the inhibition of $S1P_1$/$S1P_3$ expression or $S1P_1$/$S1P_3$-mediated signaling, because the $S1P_1$/$S1P_3$ receptors were up-regulated (Fig. 2) and the $S1P_1$/$S1P_3$-mediated Akt and ERK1/2 pathways were fully functional in senescent ECs (Fig. 4). Strikingly, $S1P_2$ receptors, which are undetected in ECs at early passages (12), were markedly induced in cultured senescent ECs (Fig. 2). The up-regulation of $S1P_2$ receptor was also observed in cultured senescent pulmonary arterial ECs (Fig. 2) as well as the lesion regions of atherosclerotic endothelium (Fig. 3), where senescent ECs were identified *in vivo* (22, 23). Importantly, ectopic expression of $S1P_2$ receptors can induce the senescent-association functional impairments in young ECs (Figs. 9 and 10). Furthermore, knockdown of $S1P_2$ receptors restores the S1P-mediated Rac activation, wound-healing, and chemotactic responses in senescent ECs (Fig. 6). Collectively, these data support the hypothesis that $S1P_2$ signaling negatively regulates chemotactic, wound-healing, and morphogenetic responses in senescent ECs. Moreover, these *in vitro* and *in vivo* lines of evidence suggest that up-regulation of $S1P_2$ receptors may be one of major risk factors involved in SA vascular dysfunctions.

$S1P_2$ signaling was shown to inhibit cell migration in the Chinese hamster ovary cells ectopically expressing $S1P_2$ receptors (15). The $S1P_2$-mediated inhibitory effect was subsequently observed in several cell lines such as mouse embryonic fibroblasts, mast cells, glioblastoma, and vascular smooth muscle cells (14, 16, 48–51). However, the $S1P_2$-mediated pathways regulating this inhibitory signaling remain to be elucidated. In this study, we show that the S1P-stimulated Rac activation is impaired in an age-dependent manner in cultured ECs (Fig. 5). ECs with different *in vitro* ages express similar amounts of Rac polypeptides (Fig. 5*A*); this suggests that the diminished Rac activity in senescent ECs is mediated by an inhibitory signal rather than a decreased expression of endogenous Rac polypeptides. Subsequently, we demonstrated that PTEN activity was markedly elevated in senescent ECs (Fig. 5*B*). Moreover, transduction with DN-PTEN restored S1P-induced Rac activation in senescent ECs (Fig. 7). These results suggest that PTEN is an essential signaling molecule in transducing $S1P_2$ signaling to mediate functional impairment in senescent ECs. In agreement, it was shown that PTEN negatively regulates Rac activation and cell migration (16). Therefore, these data together suggest that the elevated PTEN activity and reduced Rac activation may be the major factors contributing to the impaired functions in senescent ECs.

Integrin $\alpha_v\beta_3$ plays a critical role in regulating proliferation, adhesion, migration, and angiogenic responses in ECs. We recently showed that the $S1P_1$/G_i/Rho GTPase/integrin $\alpha_v\beta_3$ signaling pathway regulates the S1P-stimulated chemotactic response in young ECs (37). Although $S1P_1$ receptor-mediated signaling is fully functional in senescent ECs (Figs. 2 and 4), S1P treatment was unable to stimulate integrin $\alpha_v\beta_3$ activation in senescent ECs (Fig. 8 and supplemental Fig. S1). Also, expression of $S1P_2$ receptors in young ECs markedly inhibited S1P-

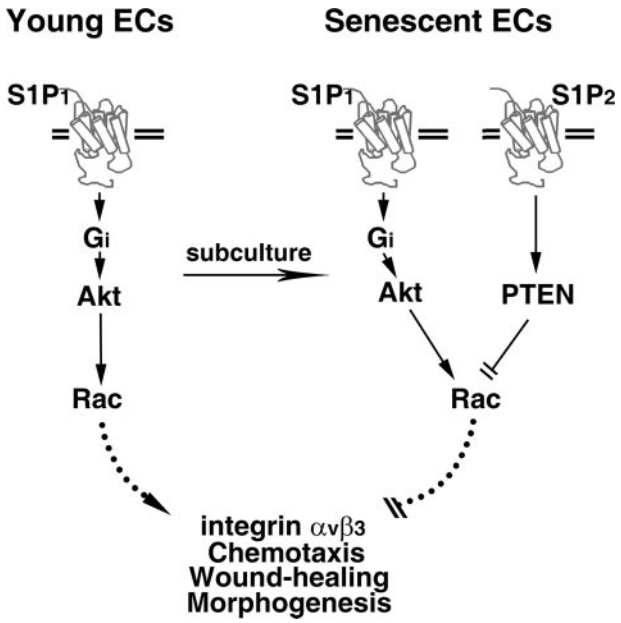

FIGURE 11. **Model for $S1P_2$ up-regulation impairs the activation of integrin $\alpha_v\beta_3$, chemotactic, wound-healing, and morphogenetic responses in senescent ECs.** $S1P_1$-mediated Akt/Rac signaling stimulates integrin $\alpha_v\beta_3$ activation, chemotactic, wound-healing, and morphogenetic responses in young ECs. In contrast, both $S1P_1$ and $S1P_2$ subtypes of S1P family receptors are up-regulated in senescent ECs. The increased expression of $S1P_2$ antagonizes the "stimulatory" signaling mediated by $S1P/S1P_1$ pathway via elevating cellular PTEN phosphatase activity. The $S1P_2$-mediated PTEN activation results in the inactivation of Rac GTPase, which ultimately inhibits the integrin $\alpha_v\beta_3$ activation, migratory, wound-healing, and morphogenetic capabilities in senescent ECs.

mediated integrin $\alpha_v\beta_3$ activation (Fig. 9*B*). These results suggest that integrin $\alpha_v\beta_3$ is one of the downstream targets of the $S1P_2$/PTEN signaling cascade. Indeed, transduction with dominant-negative PTEN in $S1P_2$-expressing young ECs markedly induced activation of integrin $\alpha_v\beta_3$ (Fig. 9*C*). Moreover, inhibition of elevated PTEN activity reinstated the S1P-induced integrin $\alpha_v\beta_3$ activation in senescent ECs. To our knowledge, this is the first demonstration of $S1P_2$/PTEN signaling negatively regulating integrin activation in vascular ECs. These data suggest that the balance between $S1P_1$ and $S1P_2$ signaling pathways may determine the functional responsiveness (such as integrin $\alpha_v\beta_3$ activation) in vascular ECs.

A "genetic programming" or "error accumulating" mechanism is thought to account for senescence-associated dysfunctions and diseases (30, 31, 38–42). Data presented in this study argue that up-regulation of $S1P_2$ receptors (*i.e.* genetic programming) negatively regulate wound-healing and morphogenetic responses of senescent ECs. Mechanistically, we demonstrated that $S1P_2$-mediated PTEN phosphatase activation results in Rac inhibition, which ultimately abrogates integrin $\alpha_v\beta_3$ activation, chemotactic, wound-healing, and morphogenetic responses in senescent ECs (Fig. 11). Indeed, knockdown of the up-regulated $S1P_2$ (Fig. 6) or inhibition of the activated PTEN (Fig. 7) restored Rac activation and functional impairments in senescent ECs. Furthermore, expression of $S1P_2$ in young ECs was replicated the SA dysfunctions that occur in senescent ECs, including impairment of integrin $\alpha_v\beta_3$ activation, chemotactic, wound-healing, and morphogenetic responses (Figs. 9 and 10). Collectively, these data suggest that $S1P_2$-mediated signaling functions as a novel switch to control the senescent-related impairments of vasculature. The knowledge obtained from this study may help develop therapeutic strategies for treating vascular dysfunctions in the future.

Acknowledgments—We thank Drs. Robert D. Gray and Binks Wattenberg for critical discussion.

REFERENCES

1. Moolenaar, W. H. (1999) *Exp. Cell Res.* **253,** 230–238
2. Spiegel, S. (1999) *J. Leukoc. Biol.* **65,** 341–344
3. Igarashi, Y., and Yatomi, Y. (1998) *Acta Biochim. Pol.* **45,** 299–309
4. Hla, T., Lee, M. J., Ancellin, N., Liu, C. H., Thangada, S., Thompson, B. D., and Kluk, M. (1999) *Biochem. Pharmacol.* **58,** 201–207
5. An, S., Goetzl, E. J., and Lee, H. (1998) *J. Cell. Biochem. Suppl.* **30–31,** 147–157
6. Zondag, G. C., Postma, F. R., Etten, I. V., Verlaan, I., and Moolenaar, W. H. (1998) *Biochem. J.* **330,** 605–609
7. Lee, M. J., Van Brocklyn, J. R., Thangada, S., Liu, C. H., Hand, A. R., Menzeleev, R., Spiegel, S., and Hla, T. (1998) *Science* **279,** 1552–1555
8. Chun, J., Goetzl, E. J., Hla, T., Igarashi, Y., Lynch, K. R., Moolenaar, W., Pyne, S., and Tigyi, G. (2002) *Pharmacol. Rev.* **54,** 265–269
9. Ancellin, N., and Hla, T. (1999) *J. Biol. Chem.* **274,** 18997–19002
10. Windh, R. T., Lee, M. J., Hla, T., An, S., Barr, A. J., and Manning, D. R. (1999) *J. Biol. Chem.* **274,** 27351–27358
11. Im, D. S., Heise, C. E., Ancellin, N., O'Dowd, B. F., Shei, G. J., Heavens, R. P., Rigby, M. R., Hla, T., Mandala, S., McAllister, G., George, S. R., and Lynch, K. R. (2000) *J. Biol. Chem.* **275,** 14281–14286
12. Lee, M. J., Thangada, S., Claffey, K. P., Ancellin, N., Liu, C. H., Kluk, M., Volpi, M., Sha'afi, R. I., and Hla, T. (1999) *Cell* **99,** 301–312
13. Lee, M. J., Thangada, S., Paik, J. H., Sapkota, G. P., Ancellin, N., Chae, S. S., Wu, M., Morales-Ruiz, M., Sessa, W. C., Alessi, D. R., and Hla, T. (2001) *Mol. Cell* **8,** 693–704
14. Goparaju, S. K., Jolly, P. S., Watterson, K. R., Bektas, M., Alvarez, S., Sarkar, S., Mel, L., Ishii, I., Chun, J., Milstien, S., and Spiegel, S. (2005) *Mol. Cell. Biol.* **10,** 4237–4249
15. Sugimoto, N., Takuwa, N., Okamoto, H., Sakurada, S., and Takuwa, Y. (2003) *Mol. Cell. Biol.* **23,** 1534–1545
16. Sanchez, T., Thangada, S., Wu, M., T. Kontos, C. D., Wu, D., Wu, H., and Hla, T. (2005) *Proc. Natl. Acad. Sci. U. S. A.* **102,** 4312–4317
17. Campisi, J. (2001) *Trends Cell Biol.* **11,** S27–S31
18. Campisi, J., Kim, S. H., Lim, C. S., and Rubio, M. (2001) *Exp. Gerontol.* **36,** 1619–1637
19. Rivard, A., Fabre, J. E., Silver, M., Chen, D., Murohara, T., Kearney, M., Magner, M., Asahara, T., and Isner, J. M. (1999) *Circulation.* **99,** 111–120
20. Albrecht, E. W., Stegeman, C. A., Heeringa, P., Henning, R. H., and van Goor, H. (2003) *J. Pathol.* **199,** 8–17
21. Sato, I., Morita, I., Kaji, K., Ikeda, M., Nagao, M., and Murota, S. (1993) *Biochem. Biophys. Res. Commun.* **195,** 1070–1076
22. Minamino, T., Miyauchi, H., Yoshida, T., Ishida, Y., Yoshida, H., and Komuro, I. (2002) *Circulation* **105,** 1541–1544
23. Minamino, T., Miyauchi, H., Yoshida, T., Tateno, K., Kunieda, T., and Komuro, I. (2004) *J. Mol. Cell Cardiol.* **36,** 175–183
24. Hannun, Y. A., and Obeid, L. M. (2008) *Nat. Rev. Mol. Cell. Biol.* **9,** 139–150
25. Rao, R. P., Yuan, C., Allegood, J. C., Rawat, S. S., Edwards, M. B., Wang, X., Merrill, A. H., Jr., Acharya, U., and Acharya, J. K. (2007) *Proc. Natl. Acad. Sci. U. S. A.* **104,** 11364–11369
26. Venable, M. E., Webb-Froehlich, L. M., Sloan, E. F., and Thomley, J. E. (2006) *Mech. Ageing Dev.* **127,** 473–480
27. Crivello, N. A., Rosenberg, I. H., Dallal, G. E., Bielinski, D., and Joseph, J. A. (2005) *Neurochem. Int.* **47,** 573–579
28. Huang, L., Grami, V., Marrero, Y., Tang, D., Yappert, M. C., Rasi, V., and Borchman, D. (2005) *Invest. Ophthalmol. Vis. Sci.* **46,** 1682–1689
29. Lee, J. F., Zeng, Q., Ozaki, H., Wang, L., Hand, A. R., Hla, T., Wang, E., and Lee, M. J. (2006) *J. Biol. Chem.* **281,** 29190–29200

30. Maier, J. A., Voulalas, P., Roeder, D., and Maciag, T. (1990) *Science* **249,** 1570–1574
31. Dimri, G. P., Lee, X., Basile, G., Acosta, M., Scott, G., Roskelley, C., Medrano, E. E., Linskens, M., Rubelj, I., Pereira-Smith, O., Peacocke, M., and Campisi, J. (1995) *Proc. Natl. Acad. Sci. U. S. A.* **92,** 9363–9367
32. Keese, C. R., Wegener, J., Walker, S. R., and Giaever, I. (2004) *Proc. Natl. Acad. Sci. U. S. A.* **101,** 1554–1559
33. Passaniti, A., Taylor, R. M., Pili, R., Guo, Y., Long, P. V., Haney, J. A., Pauly, R. R., Grant, D. S., and Martin, G. R. (1992) *Lab. Invest.* **67,** 519–528
34. Subbarao, K., Jala, V. R., Mathis, S., Suttles, J., Zacharias, W., Ahamed, J., Ali, H., Tseng, M. T., and Haribabu, B. (2004) *Arterioscler. Thromb. Vasc. Biol.* **24,** 369–375
35. Jala, V. R., and Haribabu, B. (2006) in *Methods in Molecular Biology Series* (Ali, H., and Haribabu, B., eds) Vol. 332, pp. 159–168, Humana Press, Totowa, NJ
36. Huang, J., and Kontos, C. D. (2002) *J. Biol. Chem.* **277,** 10760–10766
37. Wang, L., Lee, J. F., Lin, C. Y., and Lee, M. J. (2008) *Histochem. Cell Biol.* **129,** 579–588
38. Erusalimsky, J. D., and Kurz, D. J. (2006) *Handb. Exp. Pharmacol.* **176,** 213–248
39. Hampel, B., Fortschegger, K., Ressler, S., Chang, M. W., Unterluggauer, H., Breitwieser, A., Sommergruber, W., Fitzky, B., Lepperdinger, G., Jansen-Durr, P., Voglauer, R., and Grillari, J. (2006) *Exp. Gerontol.* **41,** 474–481
40. Erusalimsky, J. D., and Kurz, D. J., (2005) *Exp. Gerontol.* **40,** 634–642
41. Freedman, D. A., and Folkman, J. (2005) *Exp. Cell Res.* **307,** 118–130
42. Deshpande, S. S., Qi, B., Park, Y. C., and Irani, K. (2003) *Arterioscler. Thromb. Vasc. Biol.* **23,** e1–e6
43. Venable, M. E., Lee, J. Y., Smyth, M. J., Bielawska, A., and Obeid, L. M. (1995) *J. Biol. Chem.* **270,** 30701–30708
44. Ciacci Zanella, J. R., Merrill, A. H., Jr., Wang, E., and Jones, C. (1998) *Food Chem. Toxicol.* **36,** 791–804
45. Jayadev, S., Liu, B., Bielawska, A. E., Lee, J. Y., Nazaire, F., Pushkareva, M. Y., Obeid, L. M., and Hannun, Y. A. (1995) *J. Biol. Chem.* **270,** 2047–2052
46. Mouton, R. E., and Venable, M. E. (2000) *Mech. Ageing Dev.* **113,** 169–181
47. Ogretmen, B., Schady, D., Usta, J., Wood, R., Kraveka, J. M., Luberto, C., Birbes, H., Hannun, Y. A., and Obeid, L. M. (2001) *J. Biol. Chem.* **276,** 24901–24910
48. Ryu, Y., Takuwa, N., Sugimoto, N., Sakurada, S., Usui, S., Okamoto, H., Matsui, O., and Takuwa, Y. (2002) *Circ. Res.* **90,** 325–332
49. Tamama, K., Tomura, H., Sato, K., Malchinkhuu, E., Damirin, A., Kimura, T., Kuwabara, A., Murakami, M., and Okajima, F. (2005) *Atherosclerosis* **178,** 19–23
50. Lepley, D., Paik, J. H., Hla, T., and Ferrer, F. (2005) *Cancer Res.* **65,** 3788–3795
51. Yokoo, E., Yatomi, Y., Takafuta, T., Osada, M., Okamoto, Y., and Ozaki, Y. (2004) *J. Biochem.* (*Tokyo*) **135,** 673–681